Numerical Modeling and Stability Assessment of the H16 Bifurcation in the Tabas Coal Mine

Satar Mahdevari[1*]

[1]Assistant Professor, Department of Mining Engineering, Amirkabir University of Technology

ABSTRACT

The design of tunnel networks in underground mines is inherently complex, inevitably leading to various branches and intersections. The stability of these intersections directly affects the safety and efficiency of the mine. In the present study, one of the bifurcated intersections of the Parvadeh Tabas coal mine (the H16 intersection) has been investigated. The finite difference method (FLAC3D software) was employed to calculate three components: the distribution of induced stresses, the stress concentration, and the extent of the plastic zone. The results show that the maximum vertical induced stress in the area between the two tunnels reaches 25.5 MPa on the left side of the intersection. In the same zone, the stress concentration increases to 1.6 near the slope tunnel and to 1.7 near the access tunnel. At the roof of the access tunnel, moving away from the intersection is accompanied by a gradual increase in stress; a phenomenon attributed to the non-circular and wide cross-section of this tunnel. The modeling error in the three investigated sections was calculated based on the maximum displacements of 419, 412, and 370 mm, respectively, which correspond to horizontal convergences of 838, 824, and 740 mm. The relative error of the model compared to the field data was estimated at 5%, 3%, and 8%, respectively. Due to the presence of layers with different strengths, the extension of the plastic zone at various distances from the intersection exhibits a completely asymmetric behavior. Furthermore, the presence of a coal seam at the tunnels floor not only intensifies the extent of the plastic zone but also directly leads to floor instability and heave.

KEYWORDS

Numerical modeling, Bifurcated intersection, Induced stresses, Extent of the plastic zone, Tabas mine.

1. Introduction

Underground tunnels are essential for transportation, energy, water, and mining [1–3]. In underground mines, tunnel intersections are the most critical points due to sudden geometric changes and induced stress concentrations [4,5]. Among intersection types, bifurcations (where a main tunnel splits into two branches) are particularly challenging. The middle rock pillar between the two branches experiences high compressive and shear stresses, making it the most stability-sensitive zone [6].

Numerical methods, especially the finite difference method, are widely used to analyze intersection stability [7]. Previous studies have shown that intersection angle, excavation sequence, and support systems greatly affect stability [8,9]. Combined support systems (fully grouted rockbolts, long cables, steel sets) have been proven effective [10,11]. This study investigates the H16 bifurcated intersection in the Parvadeh Tabas coal mine (slope tunnel S2 and access tunnel MG5 at ~570 m depth). The aim is to determine induced stresses, stress concentration, and plastic zone extent using FLAC3D. Model results are validated with field monitoring data,

* Corresponding Author: Email: satar.mahdevari@aut.ac.ir

and the effect of a weak coal seam at the tunnel floor on plastic zone development is evaluated.

2. Methodology

The Parvadeh coal mine, the first mechanized coal mine in Iran, has an annual production capacity of about 2.5 million tonnes of raw coal [12]. The study area consists of mudstone, siltstone, sandstone, and coal seams (B1, B2, C1, C2, D), with seam C1 being the most important in terms of thickness and stability [13]. The investigated H16 bifurcated intersection connects the slope tunnel S2 and the access tunnel MG5 at a depth of about 570 m with an intersection angle of 78°. The slope tunnel has a D-shaped cross-section (width 5.6 m, height 3.95 m), which gradually widens to a trapezoidal shape (width 6.9 m) at the intersection. The access tunnel initially has an irregular trapezoidal cross-section at the intersection, then transitions to a regular trapezoid and finally to a D-shaped section.

A finite difference method using FLAC3D software was used to simulate the rock mass behavior around the H16 intersection. The model dimensions (100×70×100) were determined based on the Saint-Venant principle (five times the tunnel width) to minimize boundary effects [14,15]. The in-situ stress ratio (horizontal to vertical) was set to K=1.15 based on field measurements. The Mohr-Coulomb constitutive model was adopted, and the staged excavation sequence followed the actual mining plan. The proposed support system includes fully grouted rockbolts (22 mm diameter, 2.4 m length), long cable anchors (9 m), flexi-bolts (6 m), steel sets (TH36, IPB260, IPB320), and wire mesh. Model validation was performed using field monitoring data from three sections (2792, 2795, 2798) over five months. The maximum horizontal displacements were 419, 412, and 370 mm, corresponding to relative errors of 5%, 3%, and 8%, respectively. These results confirm the good accuracy of the numerical model.

3. Results and Discussion

The numerical analysis shows that the maximum vertical induced stress (25.5 MPa) occurs on the left side of the H16 bifurcation, in the area between the slope and access tunnels. The stress concentration factor (ratio of induced stress to initial in-situ stress) reaches 1.7 near the left side of the intersection. Figure 1 presents the contours of vertical induced stress concentration in the right wall of the slope tunnel. A notable finding is that even at a distance of 23 m from the intersection center, the induced vertical stress has not returned to its initial value (14.9 MPa), indicating a wide zone of stress disturbance caused by the excavation. The three-dimensional view of induced stresses (Figure 2) clearly shows that the left side of the intersection (with a smaller angle) experiences significantly higher stress levels than the right side, with the maximum stress occurring closer to the sharp corner. The stress distribution follows a dome-shaped pattern: initially increasing, then gradually decreasing with a mild slope due to the wide extent of the disturbed zone.

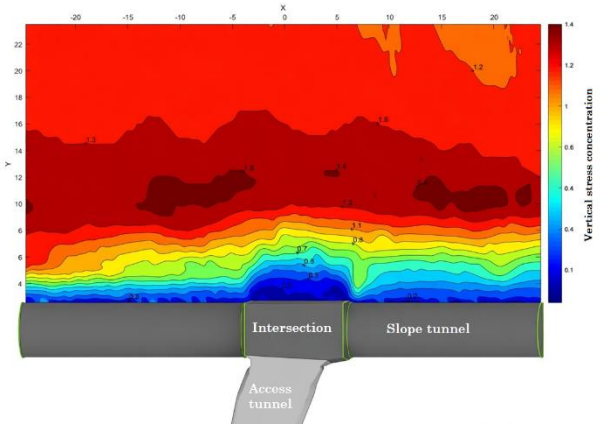

Figure 1. Contours of vertical induced stress concentration in the right wall of the slope tunnel

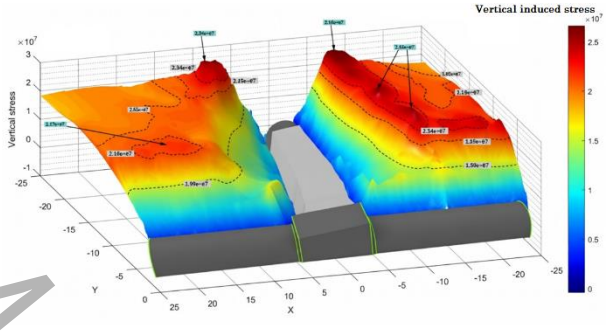

Figure 2. Three-dimensional view of vertical induced stresses on both sides of the bifurcation intersection

The plastic zone around the bifurcation exhibits a strongly asymmetric behavior, primarily due to the presence of alternating stiff and weak rock layers. As shown in Figure 3, before excavation of the access tunnel, the plastic zone is concentrated mainly at the crown and floor of the inclined tunnel. After excavation of the access tunnel, the plastic zone expands significantly, especially in the floor (up to 8.7 m depth) compared to the crown (about 5.7 m). This asymmetry becomes even more pronounced at the intersection itself. In some areas, the plastic zone extends up to 14 m on the obtuse-angle side and more than 16 m on the acute-angle side of the middle rock pillar, while in other regions it remains limited to 8–9 m. These results confirm that the local geology and excavation sequence directly control the yielding mechanism.

The position of the weak coal seam relative to the tunnel cross-section plays a decisive role in plastic zone development. When the weak layer is located in the tunnel roof, its influence on plastic zone expansion is limited. However, when the weak coal seam is present at the tunnel floor, the plastic zone expands dramatically downward, leading to severe floor instability and heave.

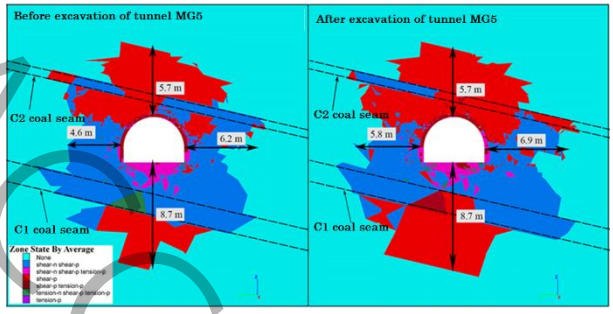

Figure 3. Plastic zone at distances of 15 m before and after excavation of the access tunnel

This finding is critical for deep coal mines. Therefore, numerical modeling must accurately incorporate geological layering, and support system design should pay special attention to floor conditions. Measures such as deep floor anchors, increasing floor bearing capacity, and combined support systems (fully grouted rockbolts, long cables, and steel sets) are recommended to control plastic zone development and enhance long-term stability of bifurcated intersections.

4. Conclusion

In this study, the stability of the H16 bifurcated intersection in the Parvadeh Tabas coal mine was evaluated using the finite difference method (FLAC3D). The main numerical findings are summarized as follows: The maximum vertical induced stress in the area between the two tunnels reached 25.5 MPa on the left side of the intersection, which is 1.7 times the initial vertical stress. The stress distribution in the rock mass between the two tunnels follows a dome-shaped pattern: it first increases and then decreases with a milder slope, indicating the wide-ranging influence of the intersection on the stress field. As the distance from the intersection center increases, the extent of the plastic zone continuously decreases in both tunnels; therefore, the most critical zone is the immediate vicinity of the intersection. The presence of inclined layers with different strengths creates an asymmetric plastic zone. The weak coal seam at the tunnel floor intensifies the plastic zone and directly leads to floor heave, whereas the same seam in the roof has little effect on plastic zone expansion. The measured convergence at various points exceeded 400 mm, and its increasing trend continued even after several months, indicating that the rock mass has not reached a stable equilibrium.

References

[1] Maidl, B., Thewes, M., and Maidl, U., 2013. Handbook of Tunnel Engineering. Wiley, Hoboken.

[2] Kolymbas, D., 2005. Tunnelling and tunnel mechanics: A rational approach to tunnelling. Springer, Berlin.

[3] Mahdevari, S., 2026. "Intelligent forecasting of tunnel deformation in underground coal mines using a dynamic swarm-tuned adaptive neuro-fuzzy inference system for knowledge-driven ground control". Advanced Engineering Informatics, 71, 104287.

[4] Liu, X., and Wang, Y., 2010. "Three dimensional numerical analysis of underground bifurcated tunnel". Geotechnical and Geological Engineering, 28(4), 447–455.

[5] Gharouni Nik, M., and Farmahini Farahani, A., 2016. "Assessment the Stability of Tunnels in Y Shaped Intersections with Regard to the Intersection Angles, Case Study: Penstock Tunnels of Rudbar Dam". Amirkabir Journal of Civil Engineering, 48(2), 191–198.

[6] Hsiao, F.-Y., Yu, C.-W., and Chern, J.-C., 2005. "Modeling the behaviors of the tunnel intersection areas adjacent to the ventilation shafts in the Hsuehshan tunnel". In World Long Tunnels, pp. 81–90.

[7] Khetwal, A., Khetwal, S., Sharma, K.G., and Panciera, A., 2023. "A 3-dimensional numerical analysis of the intersection of tunnels and shafts". In Expanding Underground-Knowledge and Passion to Make a Positive Impact on the World – Proceedings of the ITA-AITES World Tunnel Congress 2023, pp. 1608–1615.

[8] Lin, P., Zhou, Y., Liu, H., and Wang, C., 2013. "Reinforcement design and stability analysis for large-span tailrace bifurcated tunnels with irregular geometry". Tunnelling and Underground Space Technology, 38, 189–204.

[9] Chortis, F., and Kavvadas, M., 2021. "Three-Dimensional Numerical Analyses of Perpendicular Tunnel Intersections". Geotechnical and Geological Engineering, 39, 1771–1793.

[10] Xie, S., Wu, Y., Chen, D., Liu, R., Han, X., and Ye, Q., 2022. "Failure analysis and control technology of intersections of large-scale variable cross-section roadways in deep soft rock". International Journal of Coal Science & Technology, 9, 19.

[11] Wu, Y.Y., He, M.C., Li, H., Gao, Y.B., and Xie, S.R., 2024. "Instability mechanism and energy evolution of surrounding rock at intersections of deep multi-form application". Journal of Central South University, 31(3), 890–911.

[12] IRITEC, 2003. "Tabas Coal Mine Project, Detailed design report Vol 1, underground mine revision B". Technical report.

[13] Mahdevari, S., Shahriar, K., Sharifzadeh, M., and Tannant, D.D., 2017. "Stability prediction of gate roadways in longwall mining using artificial neural networks". Neural Computing and Applications, 28(11), 3537–3555.

[14] Toupin, R.A., 1965. "Saint-Venant's Principle". Archive for Rational Mechanics and Analysis, 18(2), 83–96.

[15] Timoshenko, S.P., and Goodier, J.N., 1951. Theory of Elasticity. McGraw-Hill, New York.